Colloids and Surfaces B: Biointerfaces 156 (2017) 414–421

Contents lists available at ScienceDirect

Colloids and Surfaces B: Biointerfaces

journal homepage: www.elsevier.com/locate/colsurfb

Light-triggered release from dye-loaded fluorescent lipid nanocarriers *in vitro* and *in vivo*

Redouane Bouchaala[a,b], Nicolas Anton[c], Halina Anton[a], Thierry Vandamme[c], Julien Vermot[d], Djabi Smail[b], Yves Mély[a], Andrey S. Klymchenko[a,*]

[a] CNRS UMR 7213, Laboratoire de Biophotonique et Pharmacologie, University of Strasbourg,74 route du Rhin, 67401 Illkirch Cedex, France
[b] Laboratory of Photonic Systems and Nonlinear Optics, Institute of optics and fine mechanics, University of Setif 1, 19000 Algeria
[c] CNRS UMR 7199, Laboratoire de Conception et Application de Molécules Bioactives, University of Strasbourg,74 route du Rhin, 67401 Illkirch Cedex, France
[d] IGBMC (Institut de Génétique et de Biologie Moléculaire et Cellulaire), Inserm U964, CNRS UMR7104, Université de Strasbourg, 1 rue Laurent Fries, 67404 ILLKIRCH, France

ARTICLE INFO

Article history:
Received 2 November 2016
Received in revised form 11 May 2017
Accepted 12 May 2017
Available online 15 May 2017

Keywords:
Photo-release
Controlled release
Lipid nanoemulsions
Lipophilic dyes
Fluorescence correlation spectroscopy
Fluorescence microscopy

ABSTRACT

Light is an attractive trigger for release of active molecules from nanocarriers in biological systems. Here, we describe a phenomenon of light-induced release of a fluorescent dye from lipid nano-droplets under visible light conditions. Using auto-emulsification process we prepared nanoemulsion droplets of 32 nm size encapsulating the hydrophobic analogue of Nile Red, NR668. While these nano-droplets cannot spontaneously enter the cells on the time scale of hours, after illumination for 30 s under the microscope at the wavelength of NR668 absorption (535 nm), the dye showed fast accumulation inside the cells. The same phenomenon was observed in zebrafish, where nano-droplets initially staining the blood circulation were released into endothelial cells and tissues after illumination. Fluorescence correlation spectroscopy revealed that laser illumination at relatively low power (60 mW/cm^2) could trigger the release of the dye into recipient media, such as 10% serum or blank lipid nanocarriers. The photo-release can be inhibited by deoxygenation with sodium sulfite, suggesting that at least in part the release could be related to a photochemical process involving oxygen, though a photo-thermal effect could also take place. Finally, we showed that illumination of NR668 can provoke the release into the cells of another highly hydrophobic dye co-encapsulated into the lipid nanocarriers. These results suggest dye-loaded lipid nano-droplets as a prospective platform for preparation of light-triggered nanocarriers of active molecules.

1. Introduction

Triggered release of active molecules from nanocarriers has been a subject of intensive research in the last decades [1–6]. Various triggers, such as pH, reductive potential, enzymes, temperature, ultrasound, magnetic field and light have been utilized. Light is particularly attractive in this respect, as it can be focused at a desired position of a specimen with high spatiotemporal resolution. The most common approaches for light controlled release utilize molecules that undergo light-controlled isomerization, photo-polymerization and photo-cleavage [7,8]. Thus, azobenzene *cis*-trans isomerization can trigger release from liposomes [9] polymer vesicles and micelles [10,11] and inorganic porous nanomaterials [12,13]. Photo cleavage reactions in *o*-nitrobenzyl [14–16], coumarin [17], spiropyran [18,19], malachite green [20], cynnamic acid [21,22] derivatives, etc can produce photo-driven hydrophobicity and charge changes, polymer/lipid fragmentation and de-crosslinking. However, majority of examples of the light-triggered release from nanocarriers reported to date require UV light or two-photon excitation [17,23]. The other approach utilizes surface plasmon and photo-thermal effects, to trigger the cargo release. In this case, most commonly gold nanoparticles, nanorods or nano-shells, are used in combination with polymer, lipid nanocarrier or thermo-sensitive covalent bonds [24–28]. The plasmon absorption in these nanostructures was successfully tuned, so that they could be activated with almost any desired excitation wavelength from UV up to near-infrared (NIR) region [29,30]. However, photothermal effects using gold nanostrcutures generally require relatively strong illumination powers [31], which can be harmful for the biological sample. Upconverting nanoparticles, which convert NIR light into visible and further produce photochemical effect should be also mentioned, but so far all exam-

* Corresponding author.
E-mail address: andrey.klymchenko@unistra.fr (A.S. Klymchenko).

http://dx.doi.org/10.1016/j.colsurfb.2017.05.035
0927-7765/

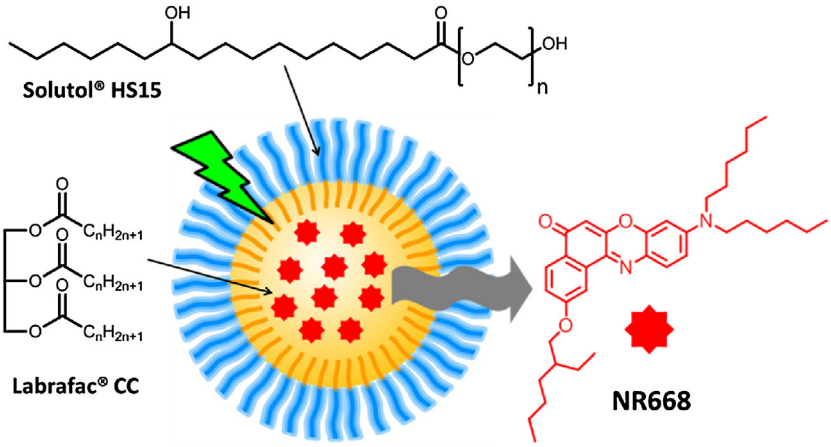

Fig. 1. Concept: lipid nanocarrier and the effect of light on the encapsulated Nile Red derivative NR668.

ples of photo-release with upconversion nanoparticles are limited to inorganic systems [32,33]. In order to develop organic photo-responsive systems one should use dyes encapsulated inside a nanocarrier. In this case, dyes operate as photosensitizers generating highly reactive singlet oxygen and/or as converters of light energy into heat. As photosensitizers, organic dyes, due to their capacity to disrupt biological membranes, were used for photochemical delivery into the cells of molecules and nanoparticles [34–37]. The use of organic dyes as triggers of molecular release from a nanocarrier were mainly realized in lipid vesicles, where local photothermal or photochemical effects were proposed as driving mechanisms of photo-release [38–42]. The photothermal effects were also reported for NIR dyes loaded into nanocarriers in cancer therapy applications [43–45].

Lipid nanoemulsions are an important nanocarrier platform, as they can be readily prepared from FDA approved agents and their hydrophobic core can encapsulate drugs and contrast agents [46–50]. Previously, the group of Texier suggested these lipid nanocarriers as imaging agents by loading their core with apolar cyanines [51,52]. We further suggested a particular probe design, using long alkyl chains and bulky hydrophobic counterions, that can increase the dye encapsulation together with preservation of the highly efficient fluorescence [53,54]. Moreover, recent FRET- based studies revealed their high stability *in vitro* and *in vivo* and capacity to enter tumors in the intact form [55,56]. In particular, we showed that the use of highly hydrophobic substituents of Nile Red enables to significantly increase dye loading, preserve good fluorescence efficiency and drastically decrease the dye leakage [53]. However, the question remained: can a strong illumination of a large quantity of dyes confined on the nanoscopic space destabilize lipid droplets? This point was not studied up to now owing to the difficulty to encapsulate a large amount of dyes in these nanoscale reservoirs. Taking recently proposed approaches [53,54], the dye concentration can be increased up to 5 wt% along with conserving their fluorescent properties. This is precisely the point that can open the door to photo-triggered properties. Although Nile Red photosensitizing properties were not described yet, we have shown earlier that large concentrations of Nile Red-based membrane probe (NR12S) can produce some photo-damage on cell membranes [57], which suggests that Nile Red as photo-active molecule to destabilize lipid nanocarriers.

In the present work, we describe an unexpected phenomenon, which is the light-triggered release of nano-droplet content, when encapsulating a hydrophobic Nile Red analogue. We show that the dye release can be observed both in cell culture and *in vivo* on a zebrafish model. The light-induced dye release was validated with different acceptor media, such as blank nanocarriers and 10% serum and it can be inhibited in the presence of oxygen scavenger. Finally, the light-driven release of a co-encapsulated molecule (second encapsulated dye) along with the Nile Red derivative was validated, which proposes the route to light-controlled drug release from lipid nano-droplets.

2. Results and discussion

The idea of light-triggered release from nano-carrier is summarized in Fig. 1. The nano-emulsion droplets can be considered as reservoir with high local concentration of dyes. Our question was whether illumination of this large ensemble of dyes within the small volume of lipid nanocarrier could produce release of its content due to photophysical or photochemical phenomena. As a dye for encapsulation, we selected a derivative of Nile Red bearing long alkyl chains (NR668, Fig. 1). Although this dye is expected to be cell permeant (like parent Nile Red), its high hydrophobicity ensures encapsulation into nano-droplets with minimal leakage effects, which prevents its fast accumulation in the cells [53].

We first prepared nanocarriers by spontaneous emulsification of Solutol, Labrafac and NR668 dye in water, which gave 32 nm particles of low polydispersity index (<0.1) according to dynamic light scattering. The phenomenon of dye release under light illumination was first studied in cell culture. Solutol® (Kolliphor®) HS 15/Labrafac® WL nanoemulsions loaded with hydrophobic Nile Red derivative NR668 was incubated with cells and studied by wide-field fluorescence microscopy. Our earlier works showed that no internalization was observed for the same system even after 2 h of incubation with HeLa cells [53], which showed that these nanocarriers cannot enter the cells on this time scale. Therefore, this system is ideal for testing the effect of light, as no artifacts due to particle internalization or dye leakage into the cells was observed. After 30 min of incubation of the cells with the emulsion of nanocarriers containing 1 wt% of NR668, the cells remained poorly fluorescent, as the fluorescence of the medium was more intense than that of the cells. Moreover, after washing of the cells, no significant fluorescence was detected inside the cells (Fig. S1), which confirmed that NR668 nano-droplets did not spontaneously internalize within this time scale. Then, we illuminated the cells surrounded by NR668-loaded nanocarriers for 30 s at 535 nm (absorption maximum of NR668 in nano-droplets is 526 nm [53]) using the maximal lamp power (~14 W/cm^2 power density at the sample level). The light action resulted in a strong photobleaching of the area of observation. Indeed, it was observed that initially very bright fluorescence field became non-fluorescent after the illumination (Fig. 2). Then,

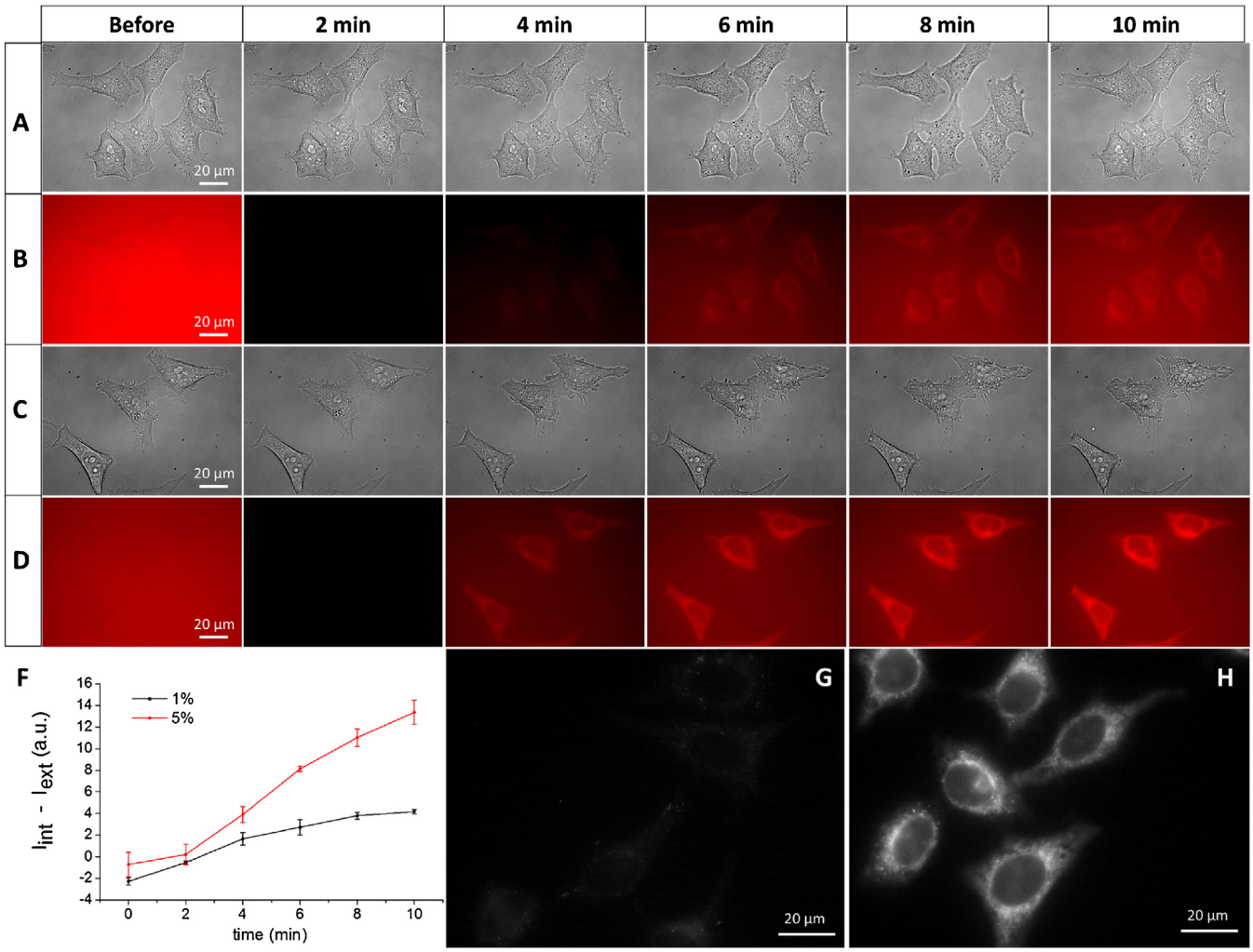

Fig. 2. Release of dye molecules *in vitro*. Brightfield (A and C) and fluorescence (B and D) images of Hela cells in the presence of nanocarrier loaded with at 1% (A, B) or 5% (C, D) of NR668. The first images on the left correspond to samples before illumination, while all others are after illumination for 30 s at 535 nm with 2 min delay for each consecutive image. All the experiments were done at 37 °C. (F): difference between intracellular and extracellular fluorescence intensity, I_{int}-I_{ext}, vs time delay after illumination. The error bars represent the standard deviation of the mean from three independent illumination cycles ($n = 3$). (G-H) Fluorescence images after washing (from nanocarriers at 5 wt% NR668) showing non-illuminated and illuminated regions.

with time, the fluorescence of the medium started to recover, but surprisingly the fluorescence of the cells increased with time. This phenomenon was observed already at 1 wt% of dye loading and took about 10 min to achieve a clear intracellular staining (Fig. 2A and B), characterized by a significant difference between intracellular and extracellular fluorescence intensity (Fig. 2F). At 5 wt% dye loading (Fig. 2C and D), the cell staining after illumination was much stronger, so that the difference between intracellular and extracellular fluorescence intensity was >3-fold larger compared to that for 1 wt% loading. After cell washing from the nanocarriers, we could find the initially illuminated regions, where the fluorescence inside the cells was many-fold larger than that for the non-illuminated regions (Fig. 2G and H). These experiments clearly showed that nanocarriers, unable to enter the cells in the dark, can deliver the dye after illumination. It should be noted that when NR668 dye without lipid nanocarrier was added directly to the cells from its DMSO stock solution (final DMSO concentration was 1%), the intracellular fluorescence of this dye was observed (Fig. S1). Earlier works showed that its parent analogue Nile Red could also spontaneously internalize [58], which implies that plasma membrane is not really a barrier for these hydrophobic dyes. These results highlight the role of the nanocarrier, which encapsulates NR668 preventing its leakage into the cells, but ensuring its release after the illumination.

Then, we investigated whether the light-induced release can be also realized *in vivo* on zebrafish. Our earlier work showed that NR668-loaded nanocarriers remained in the blood circulation for at least 30 min without dye leakage into the endothelial cells of the vessels and surrounding tissues [53]. Here, we injected nanocarriers containing 5 wt% of NR668 and performed microscopy imaging as a function of time without and with illumination (through 450–490 nm bandpass filter). Without illumination, the red fluorescence of nano-droplets was observed exclusively inside the blood vessels for at least 60 min (Fig. 3A,B), indicating that the nanocarriers remain in the blood circulation without dye leakage into the tissues. By contrast, after the illumination, we could observe a progressive increase of the fluorescence in surrounding tissues between the blood vessels (Fig. 3C-F). The fluorescence intensity, recorded in the tissue areas showed continuous increase in time for the observation period of 60 min (Fig. 3G). Thus, the illumination triggered release of the encapsulated NR668 dye, which then diffused freely into the surrounding tissues.

To understand better the observed phenomenon of release, we performed fluorescence correlation spectroscopy (FCS) of our nanocarriers in different model biological media. FCS is a powerful

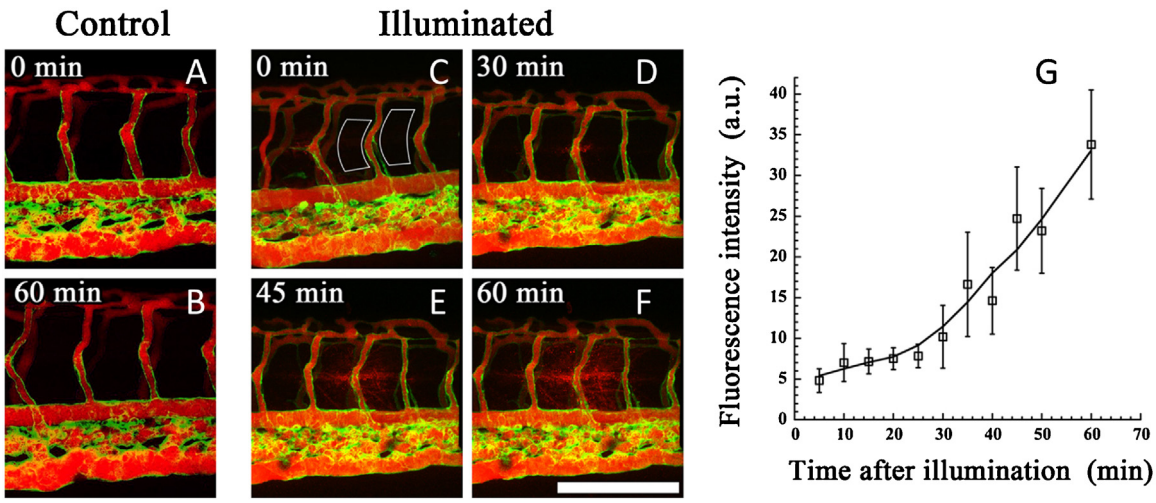

Fig. 3. The photo-induced release of the NR688 dye from the nanoemulsions in the vasculature of living zebrafish embryo. Fluorescence images of tail vasculature (green) containing NR668 nanoemulsions (red). (A,B) Control non-illuminated embryo, showing no leakage of the dye. (C-F) Embryos illuminated for 5 min through 450–490 nm bandpass filter, showing a red fluorescence in the tissues surrounding the vessels. Scale bar is 100 μm. (G) The increase in the fluorescence intensity averaged in the ROIs shown in panel (C) with time. The error bars represent the standard deviation of the mean from two different regions of the embryo ($n = 2$). (For interpretation of the references to colour in this figure legend, the reader is referred to the web version of this article.)

technique to characterize nanoparticles *in situ*, which can provide information about size, concentration and brightness of particles [53,59,60]. According to our FCS data, the particle size, measured from the diffusion correlation time of the emissive species was 33 nm (Table S1). This value is remarkably close to the hydrodynamic diameter obtained for these nanocarriers by DLS (32 nm). Moreover, the particles concentration for this sample at 1:10000 dilution, evaluated from the number of emissive species per focal volume, was 1.7 nM. Basic calculation based on known total lipid concentration in the used nanoemulsion (1.1×10^{-3}%) and the mass of a single 33-nm nano-droplet (1.9×10^{-17} g, assuming density of the droplet of 1 g/ml), we could estimate that the concentration of nanocarriers should be around 1.0 nM. The correspondence of the theoretical and experimental values of the particle concentration and the match of the particle size obtained from DLS and FCS suggest that after this 10000-fold dilution the nanocarriers remained practically intact.

In order to monitor the photo-release of the dye, we studied the number of emissive species, which, according to our earlier studies, is an important indicator of the dye release [53]. Indeed, if the dyes are released into the acceptor medium (blank particles or serum), the number of emissive species should increase (Fig. 4A). For example, in control experiments without illumination, Nile Red encapsulated into the nanocarriers showed a low number of emissive species in water and Opti-MEM, where poorly soluble Nile Red cannot really escape (Fig. 4B). On the other hand, in the presence of blank nanocarriers or fetal bovine serum (FBS), the number of emissive species increased drastically, showing that Nile Red leaked from nanocarriers and distributed in the recipient medium. By contrast, the number of emissive species for the NR668-loaded nanocarriers was low for all four studied media (Fig. 4C) and the size of emissive species remained stable (Table S1). These results confirmed our earlier data on the high stability of NR668-loaded nanocarriers against leakage [53]. After illumination with the laser at 532 nm (power density 60 mW/cm^2) the number of emissive species grew drastically in the presence blank nanocarriers and FBS, but did not change in water and Opti-MEM. The number of emissive species in the media with blank nanocarriers or FBS grew gradually on increase in the time of illumination (Fig. 4D). These results suggest that the dye photo-release is light-dose dependent and it requires a biological medium containing hydrophobic microenvironment. This was expected, because NR668 is highly apolar (log P = 9.22 [53]) and practically insoluble in water. Moreover, as the number and the size (Table S1) of emissive species in water did not change after illumination, we could conclude that illumination did not split the nanocarriers into multiple species. Therefore, the observed photo-release in the presence of the acceptor medium as well as in cell and zebrafish embryo is probably related to the light-triggered dye leakage from the nanocarriers into the surrounding hydrophobic microenvironment. The illumination also produced a drop in the total fluorescence intensity (Fig. 4E), indicating the photobleaching of the dye. The latter indicates that NR668 underwent photochemical transformation, which could explain the destabilization of the nanocarrier with further release of the dyes into the medium. Photobleaching of dyes is commonly associated with generation of singlet oxygen that further oxidize the dye or other components of the nanocarrier. Therefore, we repeated our FCS experiments in the presence of sodium sulfite. The latter is a reductive deoxygenating agent, which depletes oxygen through oxidation into a sulfate anion [61–63]. Remarkably, sodium sulfite drastically decreased the release of the dye under illumination in the presence of blank nanocarriers and serum, as it can be seen from only small change in the number of emissive species (Fig. 4C). Moreover, sodium sulfite did not show a significant influence on the fluorescence intensity of the samples before illumination (Table S1), indicating that it did not act as quencher through electron transfer or other mechanisms. Overall, these results suggest that the key mechanism that drives the dye release is linked to the photo-oxidation that could destabilize the nanocarriers.

The important question is whether illumination of NR668 can trigger release of other molecules form the nanocarriers. To this end, we encapsulated into our lipid nano-droplets a second dye, F888, which was also reported previously to remain inside the droplets without dye leakage [53], similarly to NR668. Importantly, the maxima of absorption and emission of F888 in nano-droplets at 1 wt% loading (388 and 455 nm, respectively) are well separated from those of NR668 (526 and 592 nm) [53], which should allow selective excitation and detection of three two dyes by fluorescence microscopy. We incubated the dually labeled nanocarriers with cells for 15 min and then illuminated them for 30 s at 535 nm. Before illumination, the intracellular fluorescence was weak confirming no leakage of the encapsulated dyes in the presence of cells

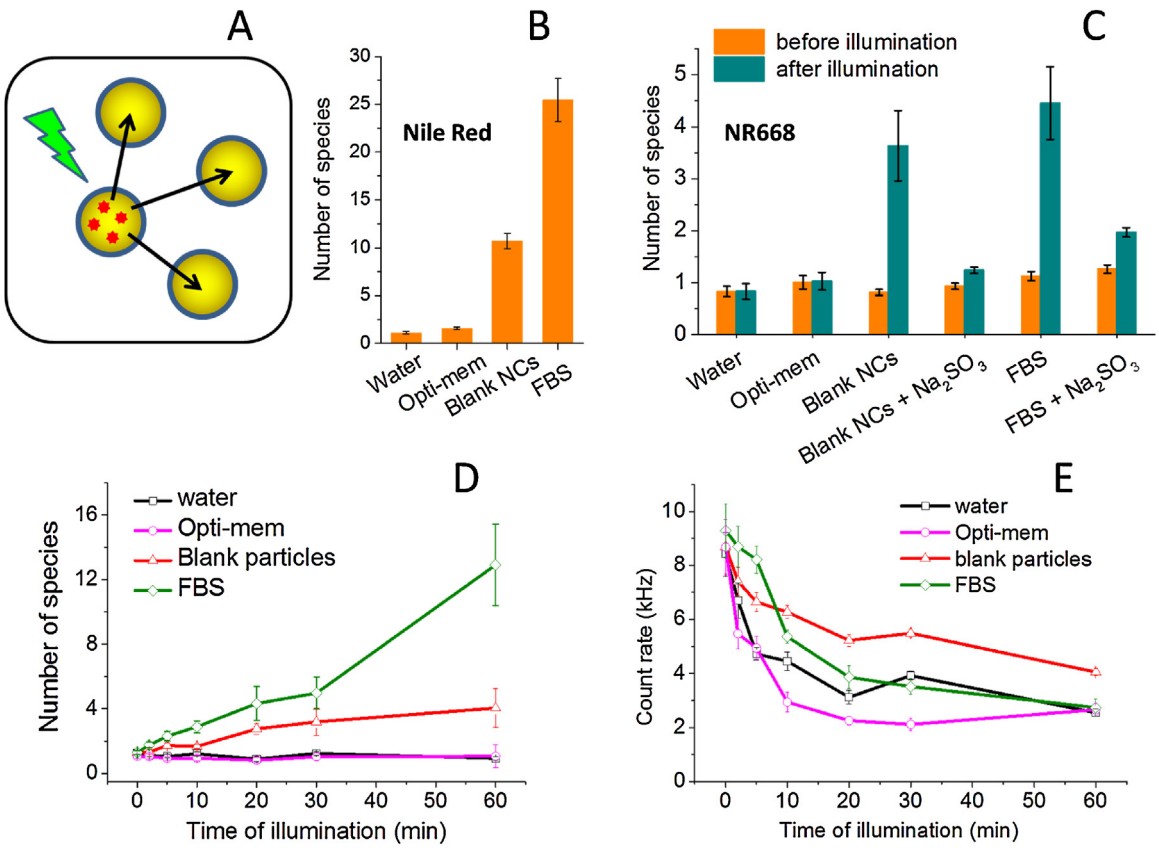

Fig. 4. Fluorescence correlation spectroscopy (FCS) studies of the light-induced dye release into model biological media. (A) Scheme explaining the effect of the dye release on the number of the emissive species. (B) Control experiment showing Nile Red dye release from nanocarriers into blank nanocarriers (NCs) and 10% serum (FBS), which was recorded as number of emissive species. (C) The effect of 30 min illumination by 532-nm laser (power density 60 mW/cm^2) on lipid nanocarriers loaded with NR668 in different media: water, Opti-MEM, blank nanocarriers and FBS. Presence of oxygen-depleting agent sodium sulfite was also tested. (D) Effect of laser illumination time on the number of emissive species and the total fluorescence intensity of NR668-loaded lipid nanocarriers in different media. The error bars in (B-E) represent the standard deviation of the mean (n = 20 recorded correlation curves).

(Fig. 5A and B). After illumination, the fluorescence recorded at the NR668 channel showed expected behavior, where the total fluorescence decreased significantly after illumination, and then increased inside the cells in the time period of 10 min (Fig. 5B). Importantly, the intracellular fluorescence recorded at the channel corresponding to F888 dye (shown in green) increased after illumination and continued increasing together with that of NR668 (Fig. 5A). Importantly, the background fluorescence in the F888 channel did not change after illumination, because this illumination cannot excite F888 dye. In the control experiment, we incubated the cells with only F888-loaded nanocarriers. After 30 s illumination at 535 nm, we found no changes in fluorescence inside the cells (Fig. S2), so that NR668 was absolutely required to induce release of F888 dye. These results showed that illumination that excites selectively NR668 dye inside nano-droplets can trigger the release of the second encapsulated dye F888. Thus, a prototype of a photo-release system is developed, where illumination of nanocarriers could induce the release of a molecule of interest, for instance in the drug delivery applications.

Finally, to clarify whether the whole nanocarrier is delivered or just its content, we incubated the cells with a mixture of nano-droplets containing separately NR668 and F888. In this case, if the whole nanocarriers enter after the illumination, then both NR668- and F888-loaded nanocarriers should be detected inside the cells. However, it was found that after illumination, only the NR668 signal was observed inside the cells, whereas the F888 signal remained low (Fig. 5C and D). This suggested that light illumination triggered the release of the dye content from NR668-loaded nanocarriers into the cells, but could not really induce internalization of the whole nanocarrier. Moreover, the fact that F888 did not enter the cells after illumination also suggested that the photo-release process did not disrupt the cell plasma membranes. This feature is important in the development of photo-release systems with minimal photo-damaging effects. Together with the FCS data, these observations suggest that the light acts at the level of the nano-droplet, producing destabilization and further cargo release into the cells. In this respect the described phenomenon is close to the light-triggered release from lipid vesicles, which was explained by photo-thermal or photochemical mechanisms [38–42]. The described phenomenon is also relevant to photochemical internalization [34–37], however, in the latter case light acts mainly at the level of cell membranes.

3. Conclusions

In the present work, a phenomenon of light-induced release from lipid nano-droplets under visible light conditions is described for the first time. It was observed using nanoemulsion droplets of 32 nm size encapsulating hydrophobic the analogue of Nile Red, NR668. These nanocarriers did not enter the cells after several hours of incubation at 37 °C, however, after illumination for 30 s under the microscope at the wavelength of NR668 absorption (535 nm), fast accumulation of the released dyes inside the cells was observed. The light-triggered release was also validated *in vivo* on zebrafish, where nano-droplets showing stable emission in the blood circulation, stained surrounding tissues after illumina-

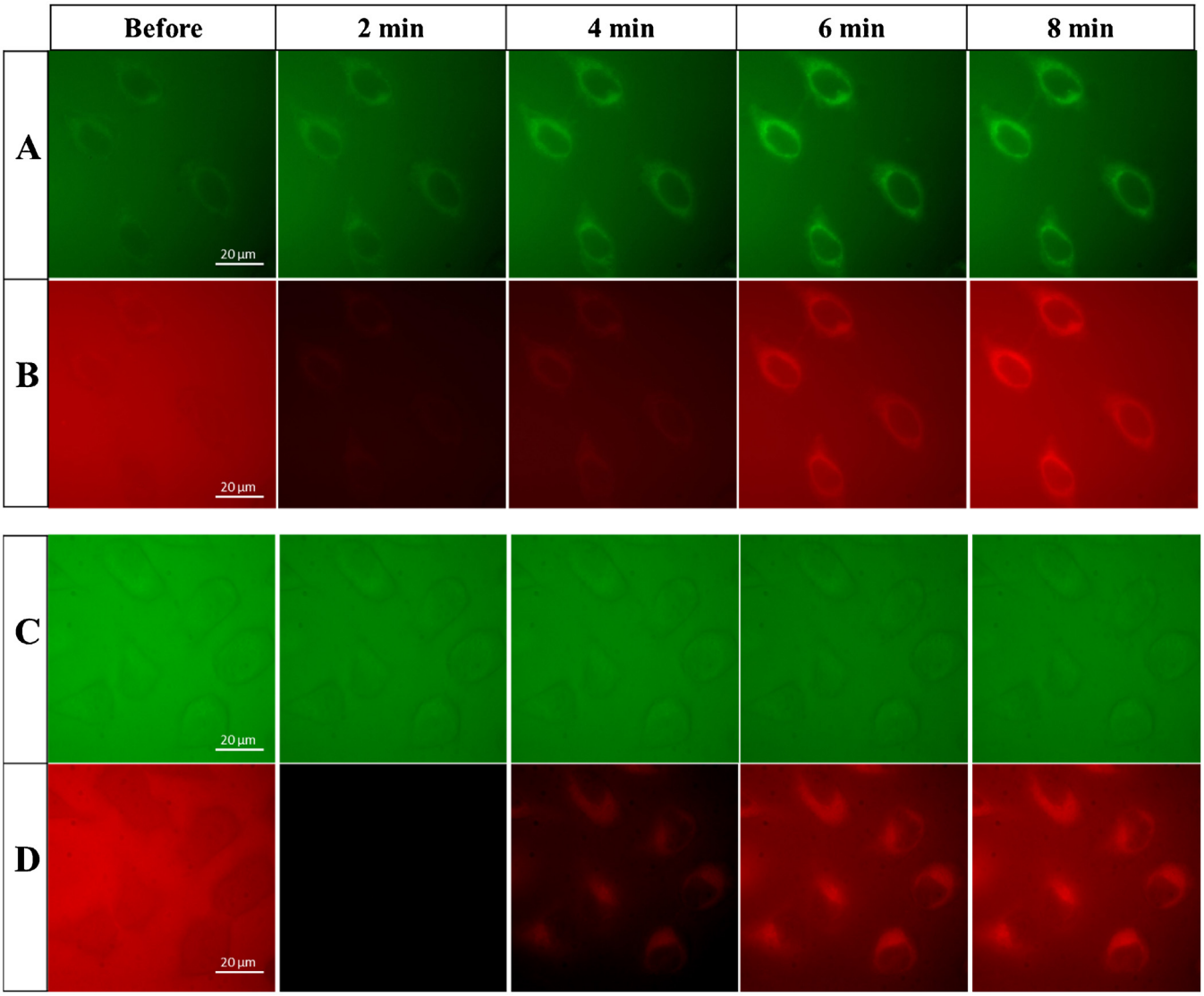

Fig. 5. Fluorescence imaging of HeLa cells incubated for 15 min at 37 °C with nanocarrier before and after illumination at 535 nm for 30 s. Images were taken every 2 min. (A and B) Nanocarriers encapsulating both dyes F888-NR668 (1 wt% each). (C and G) Mixture of nanocarriers encapsulating separately F888 (1 wt%) and NR668 (1 wt%) dyes (1:1, v:v). F888 channel: excitation 360/40 nm and emission 470/40 nm. NR668 channel: excitation 535/50 nm and emission 610/75 nm.

tion. Using fluorescence correlation spectroscopy, we showed that laser illumination at relatively low power (60 mW/cm^2) triggered dye release into 10% serum or blank lipid nanocarriers. As this process is inhibited by the deoxygenating agent sodium sulfite, we can conclude that the mechanism is linked to oxygen-dependent photochemistry, which destabilizes the nanocarrier. Nevertheless, we cannot exclude that a photo-thermal effect could also take part, as proposed in some recent literature for NIR dyes. Finally, we showed that illumination of NR668 can induce the release of another highly hydrophobic dye from the lipid nanocarriers, which was observed as accumulation of both dyes inside living cells. Based on these results, dye-loaded lipid nano-droplets emerge as a promising platform for light-triggered release of active molecules in biomedical applications. We expect that this concept could be readily extended to other dyes, which could induce under light stimulus the release of drugs from nano-droplets.

4. Materials and methods

4.1. Materials

All chemicals and solvents were purchased from Sigma-Aldrich. Kolliphor® HS15 non-ionic surfactant (mixture of polyethylene glycol 660 hydroxystearate and free polyethylene glycol 660 and) obtained from BASF (Ludwigshafen, Germany) was a kind gift from Laserson (Etampes, France), Labrafac® WL (medium chain triglycerides) was obtained from Gattefossé (Saint-Priest, France). MilliQ-water (Millipore) was used in all experiments. Culture reagents were obtained from Sigma (St. Louis, USA), Lonza (Verviers, Belgium) and Gibco-Invitrogen (Grand Island, USA). Opti-MEM® reduced serum medium was from Gibco. Dihexylamino-2-(2-ethyl-hexyloxy)-benzo[a]phenoxazin-5- one (NR668) and 4′-Dioctylamino-3-octyloxyflavone (F888) were synthesized as described before [53].

4.2. Formulation and characterization of lipid nanoparticle

Lipid nanocarriers were prepared by spontaneous nano-emulsification. Briefly, NR668 or F888 was solubilised in Labrafac® WL. Then, Kolliphor® HS 15 was added and the mixture was homogenized under magnetic stirring at 90° C. Nano-droplets of 32 nm diameter were prepared by adding 230 mg of ultrapure water to a mixture of 35 mg of Labrafac® WL and 65 mg of Kolliphor® HS 15 under intense stirring.

The size distribution of the nanoemulsions was determined by dynamic light scattering on a Zetasizer® Nano series DTS 1060 (Malvern Instruments S.A., Worcestershire, UK) and by FCS (home-built setup, see below). In the DLS measurements statistics by volume was used.

4.3. Cell culture

HeLa cells were cultured in Dulbecco's modified Eagle medium (D-MEM, high glucose, Gibco-invitrogen) supplemented with 10% (v/v) fetal bovine serum (FBS, Lonza), 1% antibiotic solution (penicillin-streptomycin, Gibco-invitrogen) in a humidified incubator with 5% CO_2 at 37 °C. Cells plated on a 75 cm^2 flask at a density of 10^6 cells/flask were harvested at 80% confluence with trypsin–EDTA (Sigma) and seeded onto a chambered coverglass (IBiDi) at a density of 0.1×10^6 cells/IBiDi. After 24 h, cells in the IBiDi dishes were washed 2 times with PBS (phosphate buffer saline) (Lonza). Then, a solution of dye-loaded nano-droplets diluted at 1: 1000 in Opti-MEM was added. Microscopy images were taken after 30-min incubation at 37 °C, unless indicated.

4.4. Microscopy

Fluorescence images were taken on a Leica DMIRE2 inverted microscope equipped with a Leica DC350FX CCD camera and a thermostated chamber (Life Imaging Services, Basel Switzerland) for maintaining the temperature at 37 °C. Cy3 filter cube (excitation 535/50 nm, emission 610/75 nm) and DAPI filter cube (excitation 360/40 nm, emission 470/40 nm) were used for detection of NR668 and F888, respectively. A 63× HCX PLAPO (1.32 NA) was used as an objective. In the photo-release studies, the illumination for 30 s was done using the same Cy3 filter cube at ~14 W/cm^2 power density of light.

4.5. Fluorescence correlation spectroscopy (FCS) and dye release

FCS measurements were performed on a two-photon platform including an Olympus IX70 inverted microscope. Two-photon excitation at 830 nm (10 mW laser output power) was provided by a mode-locked Tsunami Ti: sapphire laser pumped by a Millenia V solid state laser (Spectra Physics). The measurements were realized in an 96 well plate, using a 50 uL volume per well. The focal spot was set about 20 μm above the plate. The normalized auto-correlation function, G(t) was calculated online by an ALV-5000E correlator (ALV, Germany) from the fluorescence fluctuations, δF(t), by $G(\tau) = <\delta F(t)\,\delta F(t+\tau)>/<F(t)>^2$ where <F(t)> is the mean fluorescence signal, and τ is the lag time. Assuming that lipid nanoparticle diffuse freely in a Gaussian excitation volume, the correlation function, G(τ), calculated from the fluorescence fluctuations was fitted according to Thompson [64]:

$$G(\tau) = \frac{1}{N}\left(1+\frac{\tau}{\tau_d}\right)^{-1}\left(1+\frac{1}{s^2}\frac{\tau}{\tau_d}\right)^{-1/2} \quad (1)$$

where τ_d is the diffusion (correlation) time, N is the mean number of fluorescent species within the two-photon excitation volume, and S is the ratio between the axial and lateral radii of the excitation volume. The excitation volume is about 0.34 fL and S is about 3–4. Typical data recording times were 5 min, using dye-loaded lipid nanoparticle diluted 1: 10 000 from the originally prepared nanoparticle. Using 6-carboxytetramethylrhodamine (TMR from Sigma-Aldrich) in water as a reference, the hydrodynamic diameter, d, of nanocarriers (NCs) was calculated as: $d_{NCs} = \tau_{d(NCs)}/\tau_{d(TMR)} \times d_{TMR}$, where d_{TMR} is a hydrodynamic diameter of TMR (1.0 nm). Concentration of NCs was calculated from the number of species by: $C_{NCs} = N_{NCs}/N_{TMR} \times C_{TMR}$, using a TMR concentration of 50 nM. The data were obtained based on 20 recorded correlation curves; the recording time for each curve was 10 s for NCs and 30 s for TMR.

For the dye release studies by FCS, dye-loaded nano-droplets were diluted 10 000 fold to four different media: water, Optimem, blank nanocarriers at 1000-fold dilution (10-fold excess with respect to dye-loaded droplets) and 10% of FBS in water (serum). Each sample was placed into special 50 μl cuvette and the whole sample was illuminated with 532-nm laser at ~60 mW/cm^2 power density for different time (10 and 30 s, 10, 20 30 and 60 min) and we measure number of species and total count rate.

4.6. In vivo *studies in zebrafish*

Zebrafish were kept at 28 °C and bred under standard conditions. The transgenic line, Tg(flk1:eGFP) [65], expressing eGFP specifically in the endothelial cells, was used in order to visualize the vasculature. For the angiography, the embryos, 3 days after fertilization, were anaesthetized in egg water containing 0.04% tricaine and 0.05% phenyl thiourea (Sigma-Aldrich) and immobilized in 0.8% low melting point agarose (Sigma). The injections were performed using a Nanoject microinjector (Drummond Scientific, Broomal, PA, USA). The glass capillary was filled with NR668-loaded nanocarriers (5 wt% in oil) in 5 mM HEPES (1000-fold dilution) and 2.3 nL were injected in the sinus venosus of the embryos. The nanocarriers were immediately distributed in all the vasculature. The injected embryos were placed on the microscope stage and imaged within 5 min after injection. Intravital confocal microscopy was performed on a Leica SP5 fixed stage direct microscope with a 25× (NA 0.95) and 10× (NA 0.3) water immersion objectives. 488 nm argon laser line was used to excite both eGFP and the NR668 dyes, and their emission was detected by two separate PMTs in the spectral range 500–530 nm and 620–650 nm, respectively. At these conditions, no cross-talk between the channels was observed. The illuminations for the light-driven release were performed with a xenon lamp in epifluorescence mode using a 450–490 nm band pass filter. Confocal z-stacks and time lapses were recorded and treated by the ImageJ software (rsbweb.nih.gov/ij/). The embryos were imaged during one hour post injection and no toxicity due to the injection or to the illumination was observed. All experiments performed with zebrafish complied with the European directive 86/609/CEE and IGBMC guidelines validated by the regional committee of ethics.

Acknowledgements

This work was supported by ERC Consolidator grant BrightSens 648528. R. Bouchaala was supported by Ministry of Higher Education and Scientific Research of Algeria. We thank Ievgen Shulov for re-synthesizing NR668, L. Richert, P. Didier and F. Przybilla for help with FCS, we thank R. Vauchelles from PIQ imaging platform for help with fluorescence imaging. We also acknowledge help from the IGBMC imaging and zebrafish facilities.

Appendix A. Supplementary data

Supplementary data associated with this article can be found, in the online version, at http://dx.doi.org/10.1016/j.colsurfb.2017.05.035.

References

[1] E. Fleige, M.A. Quadir, R. Haag, Adv. Drug Deliv. Rev. 64 (2012) 866–884.
[2] S. Kaur, C. Prasad, B. Balakrishnan, R. Banerjee, Biomater. Sci. 3 (2015) 955–987.
[3] V.P. Torchilin, Nat. Rev. Drug Discov. 13 (2014) 813–827.
[4] S. Mura, J. Nicolas, P. Couvreur, Nat. Mater. 12 (2013) 991–1003.
[5] J. Liu, C. Detrembleur, S. Mornet, C. Jerome, E. Duguet, J. Mater. Chem. B 3 (2015) 6117–6147.
[6] S. Swaminathan, J. Garcia-Amoros, A. Fraix, N. Kandoth, S. Sortino, F.M. Raymo, Chem. Soc. Rev. 43 (2014) 4167–4178.
[7] N. Fomina, J. Sankaranarayanan, A. Almutairi, Adv. Drug Deliv. Rev. 64 (2012) 1005–1020.
[8] J. Olejniczak, C.-J. Carling, A. Almutairi, J. Controlled Release 219 (2015) 18–30.
[9] K. Kano, Y. Tanaka, T. Ogawa, M. Shimomura, Y. Okahata, T. Kunitake, Chem. Lett. (1980) 421–424.
[10] Y. Wang, P. Han, H. Xu, Z. Wang, X. Zhang, A.V. Kabanov, Langmuir 26 (2010) 709–715.
[11] G. Wang, X. Tong, Y. Zhao, Macromolecules 37 (2004) 8911–8917.
[12] S. Angelos, E. Choi, F. Vo, L.D. Cola, J.I. Zink, P. Institut, J. Phys. Chem. C 111 (2007) 6589–6592.
[13] Y. Tian, Y. Kong, X.J. Li, J. Wu, A.C.T. Ko, M. Xing, Colloid Surf. B-Biointerfaces 134 (2015) 147–155.
[14] J.Q. Jiang, X. Tong, D. Morris, Y. Zhao, Macromolecules 39 (2006) 4633–4640.
[15] N. Fomina, C. McFearin, M. Sermsakdi, O. Edigin, A. Almutairi, J. Am. Chem. Soc. 132 (2010) 9540–9542.
[16] X. Zhao, M. Qi, S. Liang, K. Tian, T. Zhou, X. Jia, J. Li, P. Liu, ACS Appl. Mater. Interfaces 8 (2016) 22127–22134.
[17] J. Babin, M. Pelletier, M. Lepage, J.-F. Allard, D. Morris, Y. Zhao, Angew. Chem. Int. Ed. 48 (2009) 3329–3332.
[18] H.-I. Lee, W. Wu, J.K. Oh, L. Mueller, G. Sherwood, L. Peteanu, T. Kowalewski, K. Matyjaszewski, Angew. Chem. Int. Ed. 46 (2007) 2453–2457.
[19] Q.J. Xing, N.J. Li, D.Y. Chen, W.W. Sha, Y. Jiao, X.X. Qi, Q.F. Xu, J.M. Lu, J. Mater. Chem. B 2 (2014) 1182–1189.
[20] R.M. Uda, Y. Kato, M. Takei, Colloid Surf. B-Biointerfaces 146 (2016) 716–721.
[21] M. Wang, J.-C. Kim, Int. J. Pharm. 468 (2014) 243–249.
[22] D. Shi, M. Matsusaki, M. Akashi, J. Controlled Release 149 (2011) 182–189.
[23] N. Fomina, C.L. McFearin, M. Sermsakdi, J.M. Morachis, A. Almutairi, Macromolecules 44 (2011) 8590–8597.
[24] L. Dykman, N. Khlebtsov, Chem. Soc. Rev. 41 (2012) 2256–2282.
[25] A.B.S. Bakhtiari, D. Hsiao, G. Jin, B.D. Gates, N.R. Branda, Angew. Chem. (International ed. in English) 48 (2009) 4166–4169.
[26] Y. Cheng, T.L. Doane, C.-H. Chuang, A. Ziady, C. Burda, Small (Weinheim an der Bergstrasse Germany) 10 (2014) 1799–1804.
[27] L. Paasonen, T. Laaksonen, C. Johans, M. Yliperttula, K. Kontturi, A. Urtti, J. Controlled Release 122 (2007) 86–93.
[28] W.-C. Jeong, S.-H. Kim, S.-M. Yang, ACS Appl. Mater. Interfaces 6 (2014) 826–832.
[29] X.H. Huang, I.H. El-Sayed, W. Qian, M.A. El-Sayed, J. Am. Chem. Soc. 128 (2006) 2115–2120.
[30] E. Ju, Z. Li, Z. Liu, J. Ren, X. Qu, ACS Appl. Mater. Interfaces 6 (2014) 4364–4370.
[31] Z. Qin, J.C. Bischof, Chem. Soc. Rev. 41 (2012) 1191–1217.
[32] B. Yan, J.-C. Boyer, D. Habault, N.R. Branda, Y. Zhao, J. Am. Chem. Soc. 134 (2012) 16558–16561.
[33] Y. Yang, F. Liu, X. Liu, B. Xing, Nanoscale 5 (2013) 231–238.
[34] H.L. Lu, W.J. Syu, N. Nishiyama, K. Kataoka, P.S. Lai, J. Controlled Release 155 (2011) 458–464.
[35] P.K. Selbo, A. Weyergang, A. Høgset, O.J. Norum, M.B. Berstad, M. Vikdal, K. Berg, J. Controlled Release 148 (2010) 2–12.
[36] S. Febvay, D.M. Marini, A.M. Belcher, D.E. Clapham, Nano Lett. 10 (2010) 2211–2219.
[37] A. Høgset, L. Prasmickaite, P.K. Selbo, M. Hellum, B.Ø. Engesæter, A. Bonsted, K. Berg, Adv. Drug Deliv. Rev. 56 (2004) 95–115.
[38] V.C. Anderson, D.H. Thompson, Biochim. Biophys. Acta 1109 (1992) 33–42.
[39] S.J. Leung, M. Romanowski, Theranostics 2 (2012) 1020–1036.
[40] S. Guha, S.K. Shaw, G.T. Spence, F.M. Roland, B.D. Smith, Langmuir 31 (2015) 7826–7834.
[41] K.A. Dendramis, D.T. Chiu, J. Am. Chem. Soc. 131 (2009) 16771–16778.
[42] A. Rodriguez-Pulido, A.I. Kondrachuk, D.K. Prusty, J. Gao, M.A. Loi, A. Herrmann, Angew. Chem. Int. Ed. 52 (2013) 1008–1012.
[43] J. Yu, D. Javier, M.A. Yaseen, N. Nitin, R. Richards-Kortum, B. Anvari, M.S. Wong, J. Am. Chem. Soc. 132 (2010) 1929–1938.
[44] G.T. Spence, G.V. Hartland, B.D. Smith, Chem. Sci. 4 (2013) 4240–4244.
[45] G. Chen, K. Wang, Y. Zhou, L. Ding, A. Ullah, Q. Hu, M. Sun, D. Oupický, ACS Appl. Mater. Interfaces 8 (2016) 25087–25095.
[46] D.J. McClements, Y. Li, Adv. Colloid Interface Sci. 159 (2010) 213–228.
[47] M.M. Fryd, T.G. Mason, Ann. Rev. Phys. Chem. 63 (2012) 493–518.
[48] D.J. McClements, Emulsion design to improve the delivery of functional lipophilic components, in: M.P. Doyle, T.R. Klaenhammer (Eds.), Annual Review of Food Science and Technology, vol. 1, 2010, pp. 241–269.
[49] A. Gianella, P.A. Jarzyna, V. Mani, S. Ramachandran, C. Calcagno, J. Tang, B. Kann, W.J.R. Dijk, V.L. Thijssen, A.W. Griffioen, G. Storm, Z.A. Fayad, W.J.M. Mulder, ACS Nano 5 (2011) 4422–4433.
[50] N. Anton, J.-P. Benoit, P. Saulnier, J. Controlled Release 128 (2008) 185–199.
[51] M. Goutayer, S. Dufort, V. Josserand, A. Royere, E. Heinrich, F. Vinet, J. Bibette, J.L. Coll, I. Texier, Eur. J. Pharm. Biopharm. 75 (2010) 137.
[52] I. Texier, M. Goutayer, A.D. Silva, L. Guyon, N. Djaker, I. Veronique Josserand, E. Neumann, J. Bibette, F. Vinet, J. Biomed. Opt. 14 (2009).
[53] A.S. Klymchenko, E. Roger, N. Anton, H. Anton, I. Shulov, J. Vermot, Y. Mely, T.F. Vandamme, RSC Adv. 2 (2012) 11876–11886.
[54] V.N. Kilin, H. Anton, N. Anton, E. Steed, J. Vermot, T.E. Vandamme, Y. Mely, A.S. Klymchenko, Biomaterials 35 (2014) 4950–4957.
[55] J. Gravier, L. Sancey, S. Hirsjaervi, E. Rustique, C. Passirani, J.-P. Benoit, J.-L. Coll, I. Texier, Mol. Pharm. 11 (2014) 3133–3144.
[56] R. Bouchaala, L. Mercier, B. Andreiuk, Y. Mély, T. Vandamme, N. Anton, J.G. Goetz, A.S. Klymchenko, J. Controlled Release 236 (2016) 57–67.
[57] Z. Darwich, A.S. Klymchenko, D. Dujardin, Y. Mely, RSC Adv. 4 (2014) 8481–8488.
[58] O.A. Kucherak, S. Oncul, Z. Darwich, D.A. Yushchenko, Y. Arntz, P. Didier, Y. Mely, A.S. Klymchenko, J. Am. Chem. Soc. 132 (2010) 4907.
[59] E. Haustein, P. Schwille, Fluorescence correlation spectroscopy: novel variations of an established technique Annu. Rev. Biophys. Biomol. Struct., vol. 36, 2007, pp. 151–169.
[60] D. Woll, RSC Adv. 4 (2014) 2447–2465.
[61] M.E.D. Garcia, A. Sanzmedel, Anal. Chem. 58 (1986) 1436–1440.
[62] M.A. Filatov, S. Baluschev, K. Landfester, Chem. Soc. Rev. 45 (2016) 4668–4689.
[63] S.H.C. Askes, N.L. Mora, R. Harkes, R.I. Koning, B. Koster, T. Schmidt, A. Kros, S. Bonnet, Chem. Commun. 51 (2015) 9137–9140.
[64] N.L. Thompson, in: J.R. Lakowicz (Ed.), Topics in Fluorescence Spectroscopy Techniques, vol. 1, Plenum Press, New York, 1991, p. 337.
[65] S.-W. Jin, D. Beis, T. Mitchell, J.-N. Chen, D.Y.R. Stainier, Development (Cambridge England) 132 (2005) 5199–5209.

Supplementary Material

Light-triggered release from dye-loaded fluorescent lipid nanocarriers *in vitro* and *in vivo*

Redouane Bouchaala, Nicolas Anton, Halina Anton, Thierry Vandamme, Julien Vermot, Djabi Smail, Yves Mély, Andrey S. Klymchenko

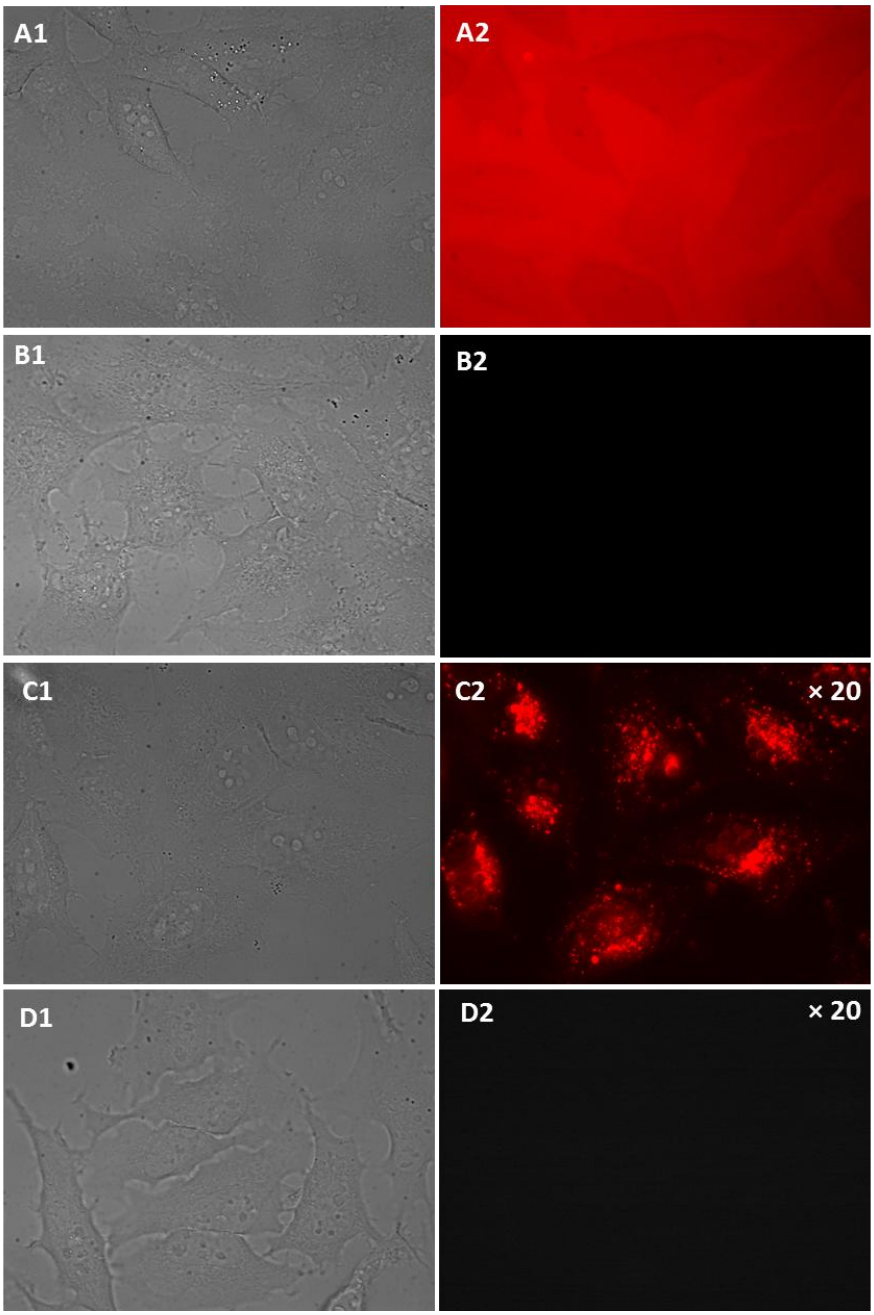

Figure S1. Bright field and fluorescence images of Hela cells. (A1-A2) NR668 nanocarriers incubated for 15 min with HeLa cells. (B1-B2) NR668 nanocarriers incubated for 15 min with cells then washed by PBS. (C1-C2) NR668 without nanocarriers (added from DMSO) incubated for 15 min with cells. The signal in C2 is multiplied 20-fold for visibility. All experiments were done at 37 °C. (D1-D2) Control image of HeLa cells without NR888 using the same microscopy settings. The size of the images was 140 × 105 μm.

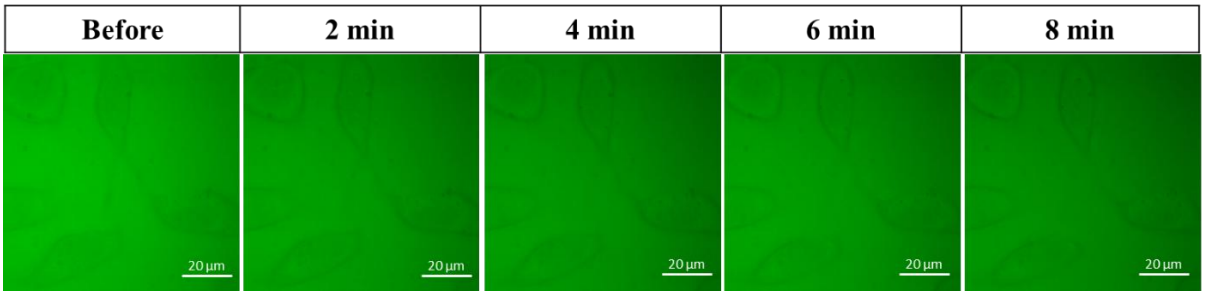

Figure S2. Fluorescence imaging of HeLa cells incubated for 15 min at 37 °C with F888-loaded nanocarrier (at 1 wt%) before and after illumination for 30 s. Each figure was taken every 2 min.

Table S1. FCS data of nanoemulsions in different media before and after illumination.[a]

Sample	**Cps (kHz)**	**N**	**τ_d (ms)**	**Chi2**	**Brightness (kHz)**	**C (nM)**	**Size (nm)**
Before illumination							
Water	32.1	0.82	1.35	0.999	38.8	1.7	33
Blank NCs	33.8	0.81	1.31	0.999	40.5	1.7	32
Blank NCs + Na_2SO_3	29.8	0.92	1.41	0.999	32.1	1.9	34
Opti-MEM	33.1	1.00	1.41	0.999	32.0	2.1	34
FBS	29.6	1.12	1.38	0.999	26.3	2.3	33
FBS + Na_2SO_3	32.1	1.26	1.42	0.999	25.6	2.6	34
After illumination							
Water	10.2	0.83	1.37	0.999	12.3	1.7	33
Blank NCs	18.6	3.63	1.28	0.998	5.11	7.5	31
Blank NCs + Na_2SO_3	13.6	1.23	1.43	0.999	11.0	2.6	34
Opti-MEM	12.1	1.02	1.39	0.998	11.9	2.1	33
FBS	17.2	4.45	1.30	0.996	3.86	9.2	31
FBS + Na_2SO_3	16.4	1.96	1.34	0.998	8.32	4.1	32
TMR (rhodamine)	67.0	24.08	0.0417	0.998	2.77	50	1.0

[a] The effect of 30 min illumination by 532-nm laser (power density 60 mW/cm^2) on lipid nanocarriers (NCs) loaded with NR668 in different media: water, Opti-MEM, emulsion of blank nanocarriers and FBS. In some samples oxygen depleting agent sodium sulphide (Na_2SO_3) was used. Cps: count rate. N: the mean number of emissive species within the two-photon excitation volume. Chi2: the goodness of the fit. τ_d: diffusion (correlation) time. C: concentration of emissive species. Size: the hydrodynamic diameter of NCs (d_{NCs}) was calculated as: $d_{NCs} = \tau_{d(NCs)} / \tau_{d(TMR)} \times d_{TMR}$, where d_{TMR} is a hydrodynamic diameter of TMR (1.0 nm). Each value is the mean of 20 recorded correlation curves (the recording time for each curve was 10 s for NCs and 30 s for TMR).